Vibration caused by swing check valve closure

Vibration caused by swing check valve closure

Aly M El-Zahaby[a], Mohamed Y Zakaria[b], Yasser A F El-Samadony[c], Ibrahim A Ismail[d,1]

[a] Professor, Mechanical Power Engineering Department, Tanta University, Tanta, Egypt.

[b] Assistant professor, Aerospace Engineering Department, Military Technical College, Cairo, Egypt.

[c] Assoc. Professor, Faculty of Engineering, Tanta University, Egypt. Also, Assoc. Professor, Faculty of Engineering, Bruit Arab University, Lebanon.

[d] PhD Student, Mechanical Power Engineering Department, Tanta University, Tanta, Egypt.

[1] corresponding author: i.a.ismail86@gmail.com

Abstract. Check valve or non-return valve is a commonly used component in fluid control systems, the function of the check valve is to allow the fluid to flow in one direction and prevent it from flowing backward in the opposite direction. There are many types of check valve that differs in structure, material, theory of operation, applications, installations constraints, etc. The swing check valve type has many advantages like lower pressure drop, high valve flow coefficient, ease of maintenance, etc. In this paper, the swing check valve type will be investigated using a new mathematical model that avoids the inaccuracy in explicit models and time consumption of evaluating different coefficients in implicit models. The present model is validated by comparing to experimental data. Investigation of the swing check valve is carried out in order to determine the vibration produced by its closing action and closing response. Also the effect of equipping the swing check valve with a torsion spring is investigated to figure out the spring effect on the valve induced vibration.

Keywords: check valve, swing, closure, fluttering, vibration, spring.

1. Introduction

Check valve is a self-operated hydraulic device that permits the fluid to flow in one direction only [1]. Different types of check valves are available [2], they differ in construction, components, theory of operation, etc. but all are built to do the same function of allowing the fluid to flow in one direction only. Examples of different types of check valve are: ball, lift, swing, diaphragm, duckbill, dual disc, tilted disc, etc., each type has advantages and disadvantages depending on the operating conditions and requirements, installation direction, used fluid, pressure drop, cracking pressure and many other criteria [3]. The swing check valve (SCV) type has low pressure drop, slurry fluids tolerance, simple construction and less need of maintenance. SCV consists of a disc/flapper hinged above the flow path, this disc opens and closes by no external aid (pilot, signal, force, etc.) but with the physical properties of both the flapper and the flow, i.e. the weight of the flapper and the hydrodynamic forces of the

flowing flow. The basic construction of the SCV is shown in Figure 1. Though the SCV has many advantages, but it also has some disadvantages like longer closing time that may cause valve slam and pressure spikes in the system that is why some SCVs are equipped with a torsion spring on the hinge to assist the closure action of the valve, reducing closing time and reversed flow, thus, reducing valve slam. Another disadvantage of the SCV is the vibration due to the closing response. Despite the vibration nowadays may be used as a good source of energy harvesting [4] either in compressible flow applications [5], [6] or in compressible flow applications [7], [8], but vibration is still a significant parameter to be taken into account when selecting a control valve.

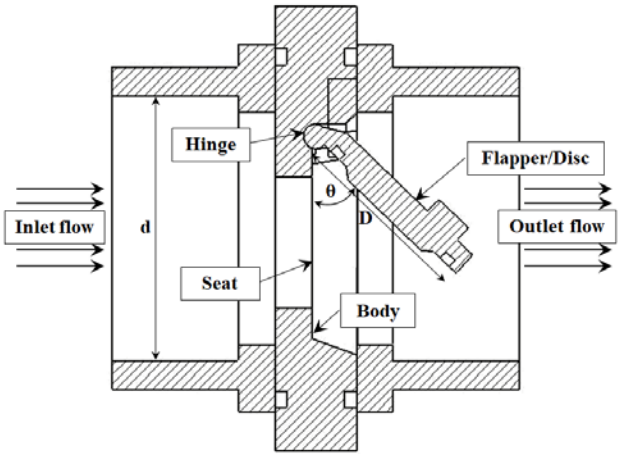

Figure 1. Basic construction of a wafer type SCV.

So, in this research a light is shed on the vibration caused by a SCV, and making use of that vibration by modifying or redesigning the SCV may be discussed in a future work.

2. Swing check valve kinematics

As previously mentioned, the SCV operation depends only on the physical properties of the flapper and the flow, so the governing forces of the SCV are the weight of the rotating flapper, the friction in the hinge, the buoyancy force, the added mass force when the flapper is accelerating, the hydrodynamic force, and finally the spring force if the valve is spring-loaded. Figure 2 shows the basic forces that govern the motion of the SCV.

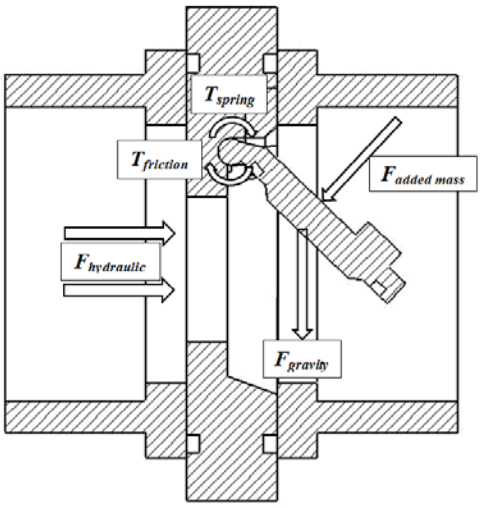

Figure 2. Basic forces on the SCV.

Because the flapper moves in an angular path around its hinge, Newton's second law for angular motion can describe the motion of the flapper as follows:

$$\sum I \,.\, \alpha = \sum T \tag{1}$$

3. Review of SCV mathematical models

The main goal of all mathematical models is to facilitate the understanding of the SCV performance, therefore, some assumptions are introduced to reduce the problem complicity and make the governing equations solvable, but without violating the accuracy concern. These assumptions are mainly: the closing time of the upstream valve is longer than its critical closing time, to avoid water hammer phenomenon, and the flow is fully developed, incompressible, adiabatic and isothermal.

Rahmeyer [9] built his steady-state model that calculates both the SCV flapper's angle with its seat at different flow velocities, and the minimum flow velocity required to fully open the SCV without fluttering (v_{min}). The author considered the hydraulic torque effect in two components: the first is the pressure difference across the valve disc and the other is the flow impingement force on the flapper's projected area. Rahmeyer experimentally examined several SCVs to introduce his new concept about the pressure drop coefficient (k_b) in water and to determine its value:

$$I_{Flap}.\alpha = T_w + T_H \tag{2}$$

$$T_H = T_v + T_p \tag{3}$$

$$T_w = W_{disc}.L.B.\sin\theta \tag{4}$$

$$T_v = A_{proj}.\rho.v^2.\cos\theta\,.\left[h + \frac{z}{2}\right] \tag{5}$$

$$T_p = \frac{\pi}{4}.D^2.L.\rho.v^2.(k_b.\theta)^{-3} \tag{6}$$

Where (B) is the buoyancy correction factor:

$$B = \frac{\gamma_{dsic} - \gamma_{fluid}}{\gamma_{disc}} \tag{7}$$

And

$$h = \frac{\left[L - \frac{d}{2}\right]}{\cos\theta} \tag{8}$$

$$z = \left[L + \frac{D}{2}\right] - h \tag{9}$$

Where k_b=0.035 for v_{min} calculations and 0.025 for angle versus velocity calculations.

Botros et al. [10] modified Rahmeyer's calculations of the flapper's projected area (A_{proj}) and also the coefficient of pressure drop value (k_b) to be valid for compressible fluids, equation (14).

$$I_{Flap}.\alpha = T_w + T_H + T_f \tag{10}$$

$$T_H = T_v + T_p \tag{11}$$

$$T_w = W_{disc}.L.B.\sin\theta \tag{12}$$

$$T_v = A_{proj}.\rho.v^2(L - y_c) \tag{13}$$

$$k_b = 0.02368 + 3.942 * 10^{-17}\theta^8 \tag{14}$$

$$T_p = \frac{\pi}{4}.D^2.L.\rho.v^2.(k_b.\theta)^{-3} \tag{15}$$

$$c = L(1 - \cos\theta) \tag{16}$$

$$y' = \frac{-c+\sqrt{c^2-\tan^2\theta.(\frac{d^2}{4}-\frac{D^2}{4}-c^2)}}{\tan^2\theta} \tag{17}$$

$$y_c = \frac{M_1+M_2}{A_{proj}} \tag{18}$$

$$M_1 = \frac{2}{3}\left(\frac{d^2}{4} - (y'-c)^2\right)^{\frac{3}{2}} \tag{19}$$

$$M_2 = \frac{2}{3}\cos^2\theta.\left(\frac{D^2}{4} - \frac{y'^2}{\cos^2\theta}\right)^{\frac{3}{2}} - \frac{\pi c D^2}{8}\cos\theta + y'c\sqrt{\frac{D^2}{4} - \frac{y'}{\cos^2\theta}} + \frac{cD^2}{4}\cos\theta.\sin^{-1}(\frac{2y'}{D\cos\theta}) \tag{20}$$

Lim et al. [11] also modified Botros' approach for calculating A_{proj} but used Rahmeyer's coefficient of pressure drop (k_b) in water to modify the SCV model in MARS code as follows:

$$I_{Flap}.\alpha = T_w + T_H + T_f + T_{damp} \tag{21}$$

$$T_H = T_v + T_p \tag{22}$$

$$T_w = W_{disc}.L.B.\sin\theta \tag{23}$$

$$T_p = \frac{\pi}{4}.D^2.L.\rho.v^2.(k_b.\theta)^{-3} \tag{24}$$

$$T_v = \rho v^2(L.A_{proj} - \oint_{A_{proj}} .y.dA) \tag{25}$$

$$y_c = \frac{c-\cos\theta\sqrt{c^2+\sin^2\theta.(R_{disc}^2-R_{pipe}^2)}}{\sin^2\theta} \tag{26}$$

$$c = L(1-\cos\theta) \tag{27}$$

$$\oint_{A_{proj}} y.dA = \frac{2}{3}\left(R_{pipe}^2 - y_c^2\right)^{\frac{3}{2}}(1+\cos^2\theta) + c\left[\frac{1}{2}\pi R_{dsic}^2.\cos\theta - R_{dsic}^2.\sin^{-1}\left(\frac{c-y_c}{R_{disc}.\cos\theta}\right)\cos\theta - (c-y_c)\times\sqrt{R_{pipe}^2 - y'^2}\right] \tag{28}$$

$$y' = \frac{-c+\sqrt{c^2-\tan^2\theta.(\frac{d^2}{4}-\frac{D^2}{4}-c^2)}}{\tan^2\theta} \tag{29}$$

$$T_f = \Delta p_{cr}.A_{disc}.L \tag{30}$$

$$T_{damp} = C_{damp}.D^5.\omega^2 \tag{31}$$

Unlike the past steady-state explicit models, A new implicit and more accurate model was introduced by Li and Liou [12], where the hydraulic torque was splitted into two components: the torque created by the flow around a stationary disc (T_{HS}) and the torque created by the rotation of the disc (T_{HR}):

$$\left(I_{Flap} + I_{add}\right).\alpha = T_w + T_H + T_f \tag{32}$$

$$T_w = W_S.L.\sin(\theta) \tag{33}$$

$$T_H = T_{HS} + T_{HR} \tag{34}$$

$$T_{HS} = C_{HS}.A_{disc}.\frac{1}{2}.\rho v^2.L \tag{35}$$

$$T_{HR} = C_{HR}.A_{disc}.\frac{1}{2}.\rho(L\omega)^2.L \tag{36}$$

Coefficients of the hydraulic torque and static friction torque are initially quantified (experimentally or with CFD), while the friction torque can be neglected for small valve sizes. The added mass effect of the moving flapper is considered by using the relative velocity between the flapper and the moving fluid instead of using the absolute flow velocity, and also in the moment of inertia calculations (I_{add}) as a mass occupied by a sphere shape of fluid having the same diameter of the disc:

$$m_{add} = \frac{1}{6}\rho\pi D^3 \tag{37}$$

Thus, the added mass inertia for the circular flapper will be:

$$I_{add} = m_{add}.L^2 + \frac{1}{10}\, m_{add}.D^2 \tag{38}$$

Pandula and Halász [13] as well as Tran [14] built a numerical model for the tilted disc check valve type that can be used for swing type (by neglecting the eccentricity torque). Pandula [13] used a different hydraulic torque formula, and also a different mathematical expression for friction torque:

$$I.\alpha = T_H + \cancel{T_{eccentricity}} + T_w + T_f \tag{39}$$

$$T_H = T_v + T_p \tag{40}$$

$$T_p = C_{\Delta p}(\theta).\Delta p.D_{nom}^3 \tag{41}$$

$$\Delta p = C_d(\theta).\frac{1}{2}.\rho.{v_{rel}}^2 \tag{42}$$

$$T_w = W_S.L \tag{43}$$

$$T_v = k_v.m_{disc}.D^2.(v_{rel}.L)^2 \tag{44}$$

Where:

$$v_{rel} = v_{flow} - v_{disc} \tag{45}$$

In order to solve this model, the coefficients of $C_{\Delta p}(\theta)$ and $C_d(\theta)$ must be previously measured in steady flow versus angle. The friction torque can be calculated as follows:

$$T_f = f_{bear}.F_f.\frac{1}{2}.d_{bear} \tag{46}$$

Where:

$$F_f = \sqrt{\left[\left(m_{Flap} + m_{dsic}\right)g + \left(\Delta p_{cr}.A_{disc}.sin(\theta)\right)\right]^2 + \left[\Delta p_{cr}.A_{disc}.cos(\theta)\right]^2} \tag{47}$$

The added mass effect was considered in the moment of inertia calculations as follows:

$$I = (1 + f_{add})I_{Flap} + m_{disc}.{r_{disc}}^2 \tag{48}$$

The value of added mass factor (f_{add}) ranges between (0.1 and 0.3) for positive and negative local acceleration of the disc.

Tran [14] built his model based on Li and Liou [12] model and found a relation between the C_{HR} from C_{HS} as follows:

$$C_{HR} = C_{HS}.sin(\theta)\,.\left[\frac{2v}{\omega.L} + sin(\theta)\right] \tag{49}$$

4. Present mathematical model

The present mathematical model is built based of Li [12],Tran [14] and Pandula [13] models. while the challenge of pre calculation of flow coefficients was beaten by studying the characteristics of C_{HS} that was investigated by different researchers such as Turesson [15], Boqvist [16], Björk [17], Eriksson [18] and Vavassori [19] for different SCV sizes and inlet flow velocities (v_o) in Table 1 and data is shown and Figure 3.

Table 1. Different SCVs investigations of characteristic parameters used for C_{HS}.

Parameter / Author	D_{disc} [m]	L [m]	m_s [kg]	θ_{max} [˚]	v_o [m/s]
Turesson	0.224	0.155	6.15	57	3
Boqvist	0.370	0.2553	7	58	3.5
Bjork	0.42	0.2663	7	60	3
Eriksson	0.1	0.138	0.14	59.74	2.1
Vavassori	0.370	0.2553	7.9	58	4

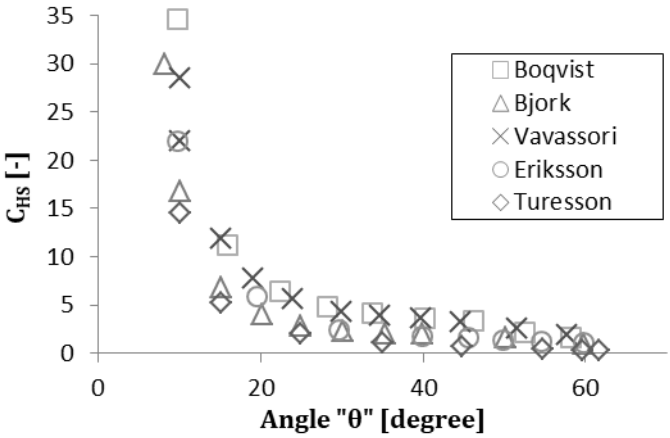

Figure 3. Different C_{HS} values versus θ.

Figure 3 shows the coefficient of the static hydraulic torque (C_{HS}) form different studies was found to have almost an average trend of:

$$C_{HS} = 2000 \times ln(\theta)^{-5} \tag{50}$$

This formula is used in the present model to get the hydraulic torque value at different opening angles.

The static friction in the flapper's hinge gave good results when calculated using Pandula's [13] method of calculating friction torque.

Tran's [14] analogy to deduce the value of the coefficient of hydraulic rotating torque (C_{HR}) was used to quantify the hydraulic torque in transient calculations. The component of the flapper's submerged

weight torque at each angle was almost the same for all models as well as present model. Finally, the spring torque is the product of the spring stiffness by the closing angle.

$$T_w = m.g.\frac{\gamma_{dsic}-\gamma_{fluid}}{\gamma_{disc}}.L.\sin\theta \quad (51)$$

$$T_H = T_{HS} + T_{HR} \quad (52)$$

$$T_{HS} = C_{HS}.\rho.A_D.L.v_{rel}^2 \quad (53)$$

$$T_{HR} = C_{HR}.\rho.A_D.L.(\omega.L)^2 \quad (54)$$

$$T_S = K\,.\theta \quad (55)$$

$$T_f = \frac{1}{2} f_{bear}.d_{bear}.F_f \quad (56)$$

$$F_f = \sqrt{[W_s + (\Delta p_{cr}.A_D.sin(\theta))]^2 + [\Delta p_{cr}.A_D.cos(\theta)]^2} \quad (57)$$

Substitute with equations (50) to (57) into Newton's second law for angular motion to solve the transient SCV model, and considering the I.α=0 for steady-state simulation.

5. Model validation

5.1. Steady-State Model

By calculating the steady-state momentum equation of the present model, we can get the flow velocity (v) at each angle as follows:

$$T_w + T_f - T_H = 0 \quad (58)$$

Then substitute with equations (51, 52 and 56) into equation (58), we get:

$$v^2 = \frac{T_w+T_f}{C_{HS}.\rho.A_D.L} \quad (59)$$

$$\therefore v = \sqrt{\frac{T_w+T_f}{C_{HS}.\rho.A_D.L}} \quad (60)$$

Starting using the MATLAB program to simulate the steady-state performance of the SCV and calculate different flapper opening angles at flow velocities with an angle step of dθ=0.25˚. Data of Rahmeyer's valve is listed in Table 2.

Table 2. Valve specifications of Rahmeyer's experiment.

Valve diameter [m]	Torque arm [m]	Submerged flapper's mass [kg]	Max. opening angle [degree]
0.333	0.189	27.37	78

Results of the present model compared to Rahmeyer [9] model and his experiment for the same swing check valve are shown in Figure 4.

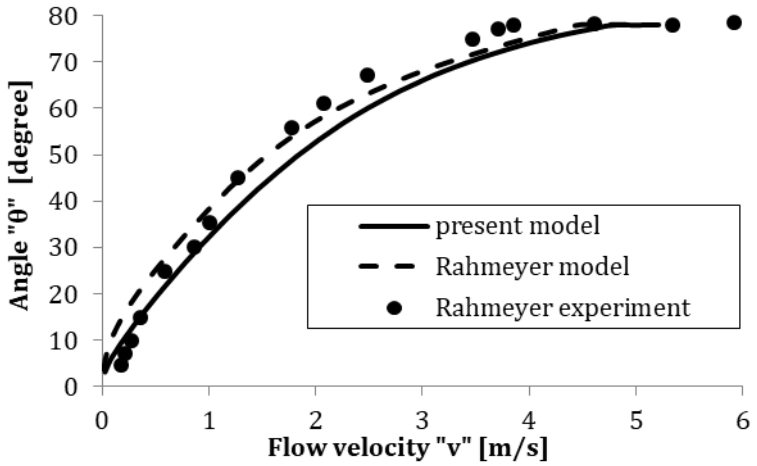

Figure 4. Opening trend of both models.

Figure 4 shows the present model having almost the same trend of Rahmeyer model with maximum error of 23.59% at θ=40˚, and a full opening velocity of v=4.84 m/s versus v=4.48 m/s of Rahmeyer's with only 8% error.

5.2. Transient model

The transient performance of the valve closure is simulated by substituting with equations (37, 38, 45, 50, 51, 52 and 56) into equation (32) and solving by MATLAB ordinary differential equation solver (ODE45).

The transient mathematical model is validated by comparing with the experimental results of Li [12], Figure 5. Data of Li's valve is listed in Table 3.

Table 3. Valve specifications of Li's experiment.

Valve diameter [m]	Torque arm [m]	Submerged flapper's mass [kg]	Flapper's moment of inertia [kg.m2]	Max. opening angle [degree]
0.07493	0.055	0.3724	0.0018	52

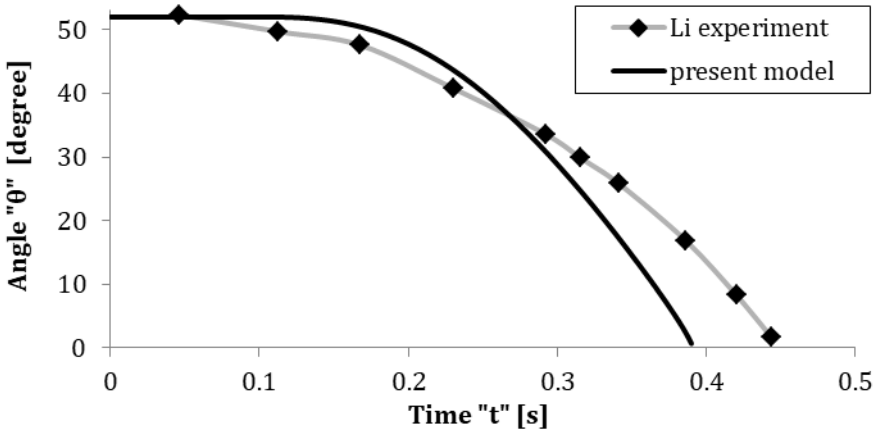

Figure 5. Present model versus Li experiment.

Though the present model does not fully lay on Li's experiment curve, but the maximum error in calculating the final closing time is about only 11.9% underestimation.

6. Results

Two cases of the SCV are examined, the first one is when no spring is attached to the SCV, and the second one when the SCV is equipped with a torsional spring with stiffness (k) of 0.5 N.m/rad. The purpose of examining the spring-loaded SCV is to check whether the spring has a good or bad effect on the vibration induced by the SCV.

6.1. Spring-free SCV

The first thing to calculate is the steady-state closing curve for Li's experiment as shown in Figure 6.

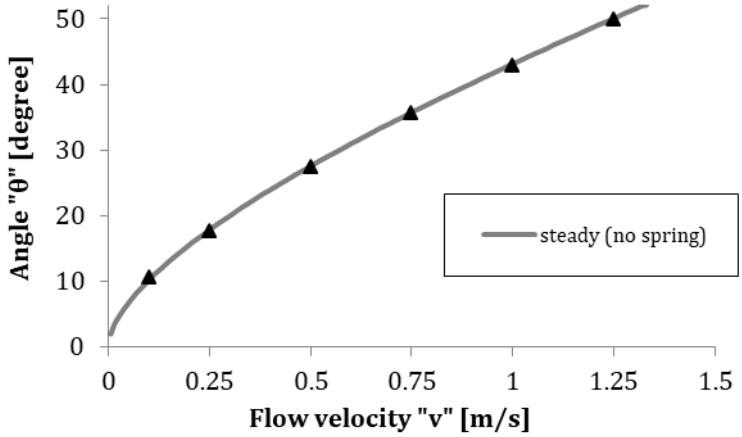

Figure 6. Steady-state pattern of flow velocity versus closing angle with no spring.

Some arbitrary values of flow velocities were selected to cover the operating range to examine the flapper's closing transient response at these values, Figure 7.

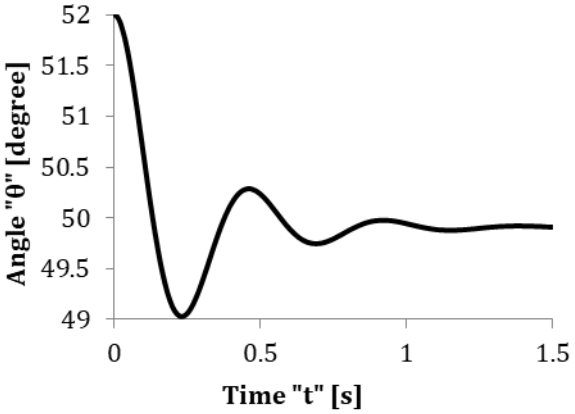

a) Transient response at v=1.25 m/s.

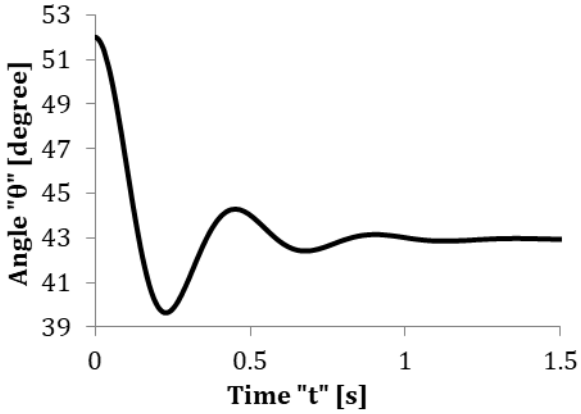

b) Transient response at v=1 m/s.

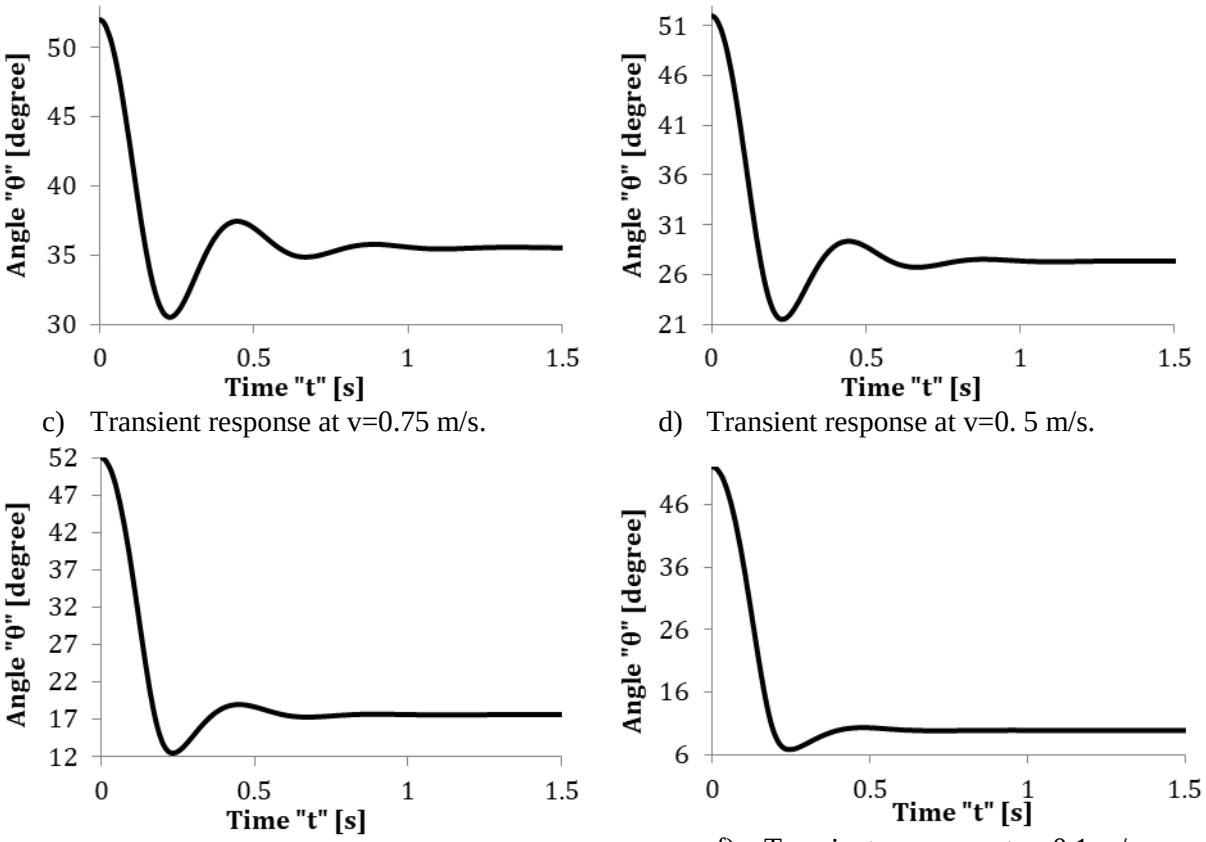

c) Transient response at v=0.75 m/s.

d) Transient response at v=0. 5 m/s.

e) Transient response at v=0.25 m/s.

f) Transient response at v=0.1 m/s.

Figure 7. Response performance of the closing angle versus time at different initial flow velocities with no spring attached.

Figure 7 shows clearly that at larger flow velocities the flapper tends to encounter much vibration than it at lower flow velocities. Larger vibration at higher flow velocities appears in lower damping ratio and higher values of overshoot, decay ration and settling time, Table 4.

Table 4. Response data at different initial flow velocities without spring.

Input velocity "v" [m/s]	0.1	0.25	0.5	0.75	1	1.25
Damping ratio "ζ"	--	0.40144	0.38649	0.31	0.30536	0.2328
Over shoot "OS"	0.1354	0.1424	0.22807	0.2922	0.32967	0.42857
Decay ratio "DR"	--	0.0636	0.0718	0.1289	0.1333	0.2222
Settling time "Ts"	0.61	0.7	0.9	1.08	1.11	1.28

For better understanding, results of Table 4 are shown in Figure 8.

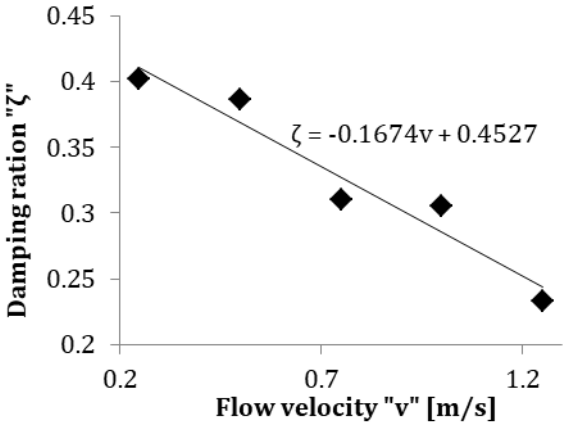

a) Damping coefficient versus flow velocity.

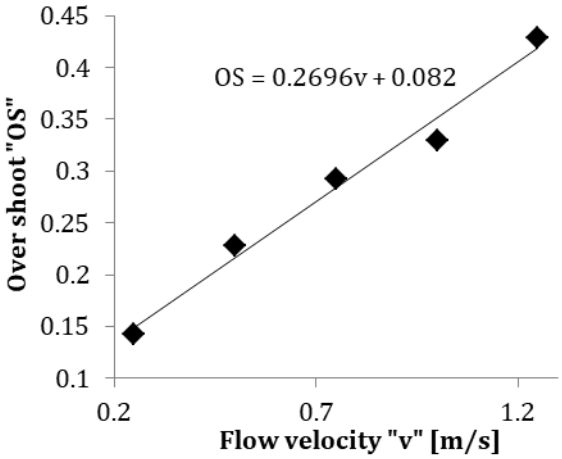

b) Overshoot versus flow velocity.

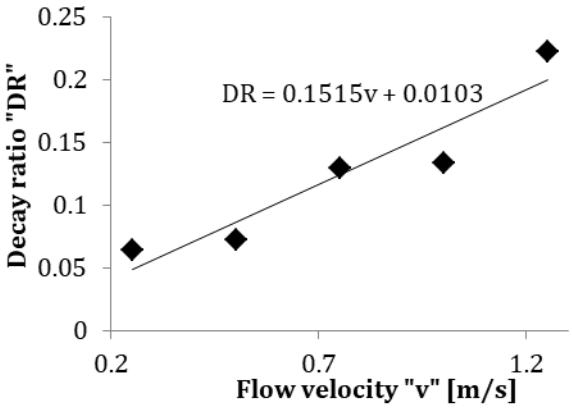

c) Decay ratio versus flow velocity.

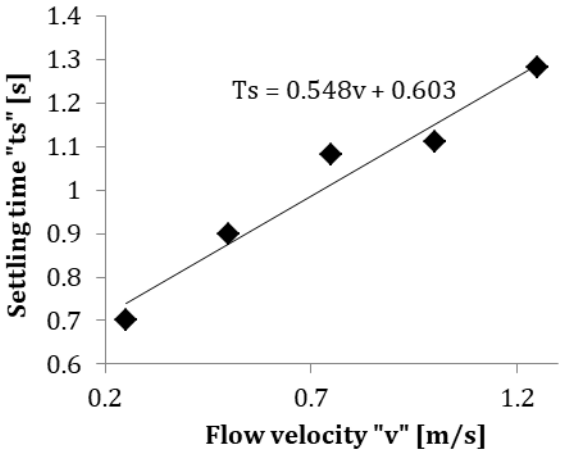

d) Settling time versus flow velocity.

Figure 8. Vibration characteristics of the spring-free SCV.

Table 4 and Figure 8 show that the larger vibration that the flapper encounter occurs at larger flow velocities, which can tell us why it is very important to calculate the minimum flow velocity required to fully open the flapper without fluttering (v_{min}) and the harm (vibration and friction) that will happen if the valve operates at values less than it.

6.2. Spring-loaded SCV

The second case is to investigate the SCV when equipped with a torsion spring with a stiffness value (k) of 0.5 N.m/rad.

The steady-state closing of the SCV is shown in Figure 9.

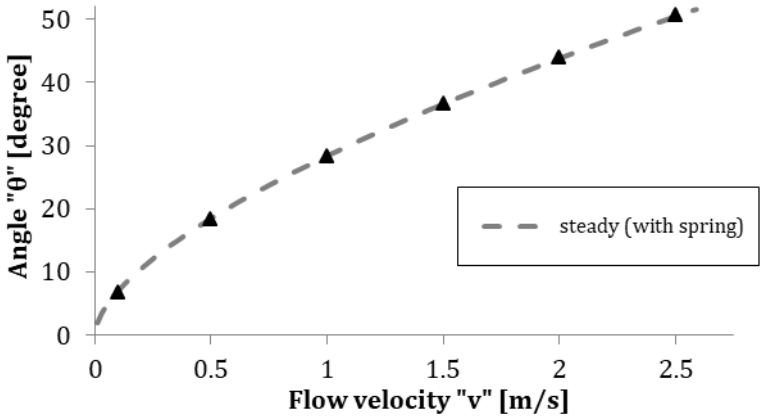

Figure 9. Steady-state pattern of flow velocity versus opening angle with spring stiffness k=0.5 N.m/rad.

It is very clear that the spring-loaded SCV requires higher value of flow velocity to fully open it, because additional torque (spring torque) is newly added here and more flow is required to overcome it.

The transient response of different values of flow velocity over the closing range is calculated and shown in Figure 10.

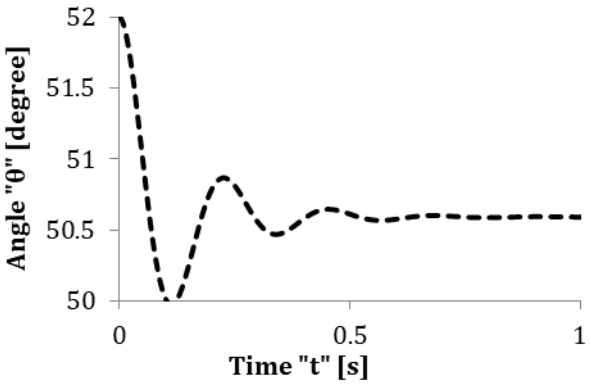

a) Transient response at v=2.5 m/s.

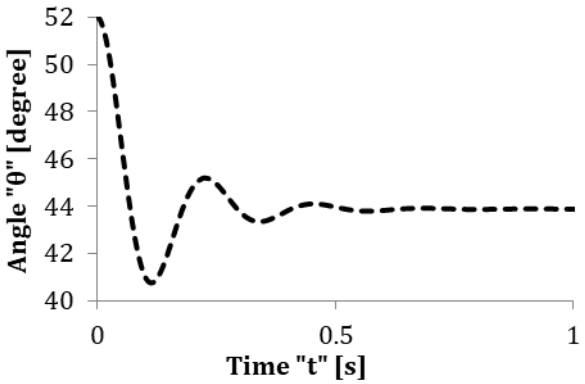

b) Transient response at v=2 m/s.

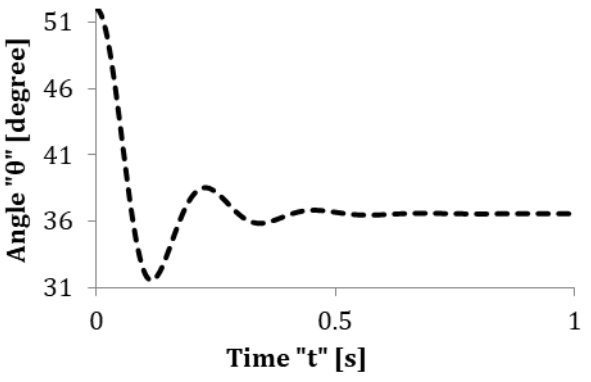

c) Transient response at v=1.5 m/s.

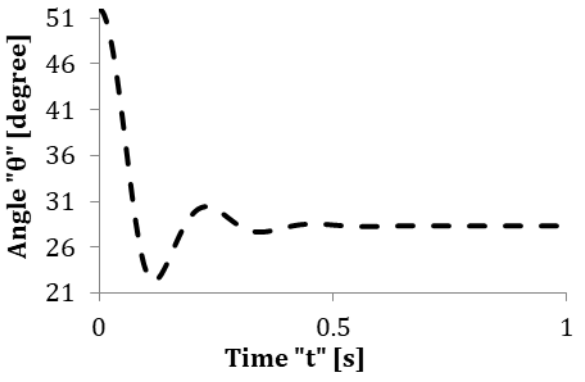

d) Transient response at v=1 m/s.

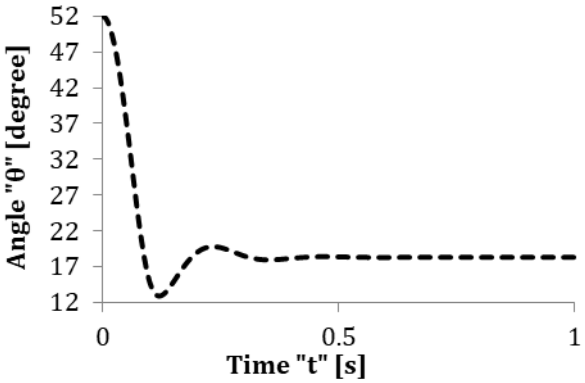

e) Transient response at v=0.5 m/s.

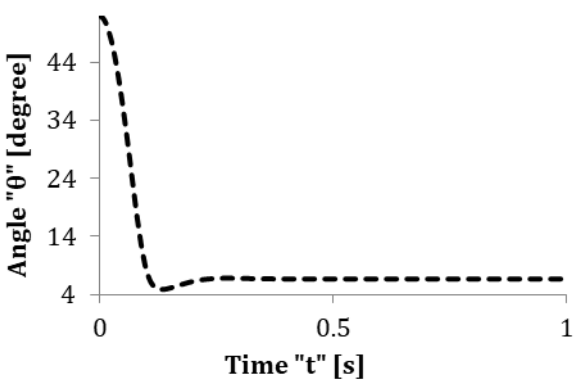

f) Transient response at v=0.1 m/s.

Figure 10. Response performance of the closing angle versus time at different initial flow velocities when a spring with stiffness of 0.5 N.m/rad. is attached.

Just like the spring-free case, Figure 10 shows that the larger values of vibration occur at larger flow velocities. Table 5 shows vibration characteristics of each flow velocity.

Table 5. Response data at different initial flow velocities with spring stiffness k=0.5 N.m/rad.

Input velocity "v" [m/s]	0.1	0.5	1	1.5	2	2.5
Damping ratio "ζ"	--	0.51302	0.33397	0.30326	0.27677	0.25825
Over shoot "OS"	0.0372	0.14849	0.23924	0.31968	0.37389	0.41844
Decay ratio "DR"	--	0.0234	0.10794	0.13539	0.1637	0.18644
Settling time "Ts"	0.25	0.43	0.47	0.53	0.57	0.69

Table 5 data are set into figures for better understanding. Figure 11 visualizes the characteristics of vibration of each flow velocity.

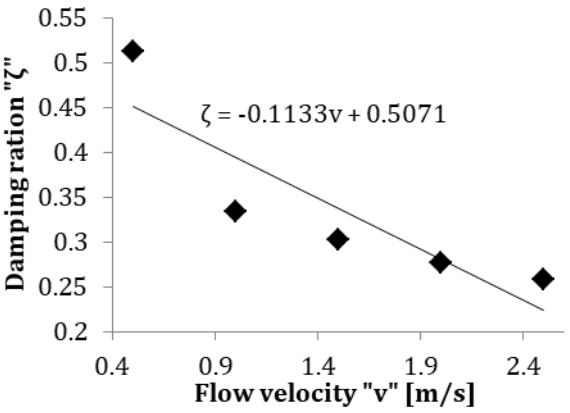

a) Damping ratio versus flow velocity.

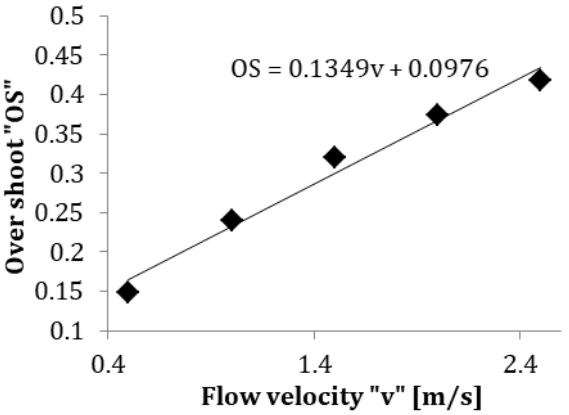

b) Overshoot versus flow velocity.

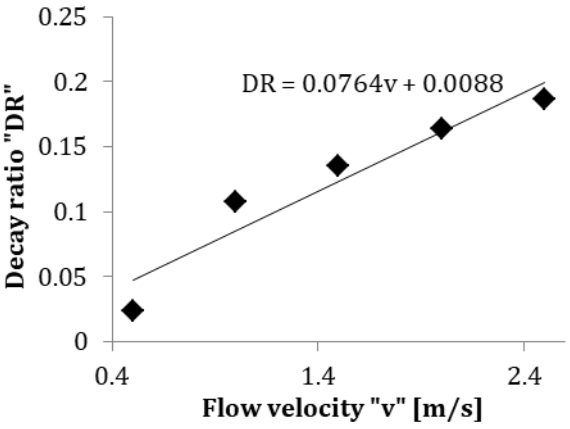

c) Decay ration versus flow velocity.

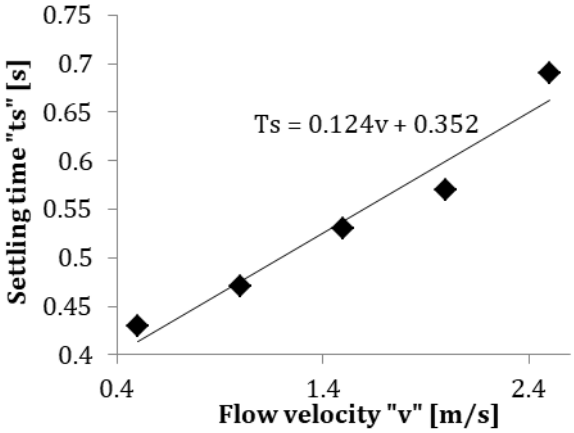

d) Settling time versus flow velocity.

Figure 11. Vibration characteristics of the spring-loaded SCV.

As well as the spring-free SCV, The spring-loaded SCV encounter larger vibration and fluttering at larger values of flow velocities.

6.3. Comparison

A comparison between the curve fitting (trend line) of both cases is summarized in Table 6.

Table 6. Curve fitting equations of different vibration properties.

	Spring-free	Spring-loaded
Damping ratio "ζ" =	-0.1674v + 0.4527	-0.1133v + 0.5071
Over shoot "OS" =	0.2696v + 0.082	0.1349v + 0.0976
Decay ratio "DR" =	0.1515v + 0.0103	0.0764v + 0.0088
Settling time "Ts" =	0.548v + 0.603	0.124v + 0.352

Table 6 shows that the trend lines of different vibration characteristics for both cases are very close, especially that one of the damping ratio. The similarity between the vibration properties performance of both cases as a function of flow velocity asserted the conclusion of the effect of spring in reducing the closing response vibration.

A worth mentioned notice when comparing the transient closure of the flapper of both cases at nearly the flow velocity at fully opened position (v_{full}) i.e. at 1.25 m/s and 2.5 m/s for the spring-free and the spring-loaded SCVs respectively, we got less vibration and fluttering when the SCV is spring-loaded despite the flow velocity is larger than the spring-free case, Figure 12. This is because the spring existence in the system bounds the vibration and the fluttering of the SCV.

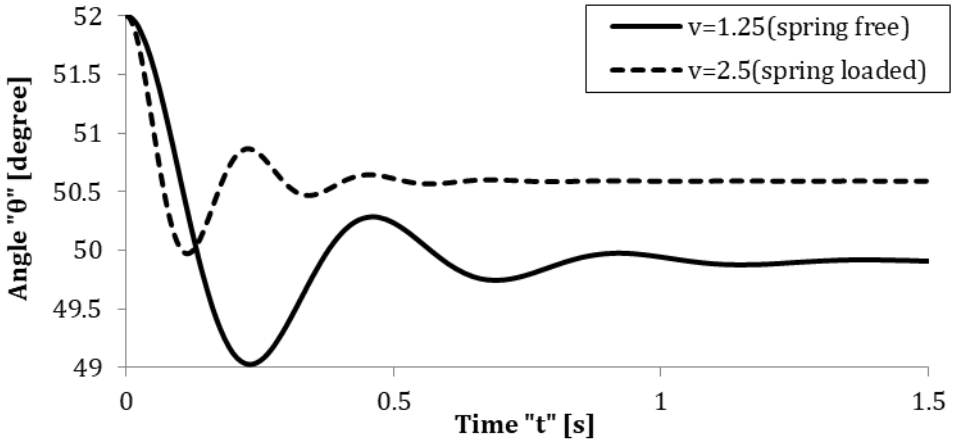

Figure 12. Transient response at nearly v_{full} for both spring-free and spring-loaded SCVs.

At the first glance at Figure 12, one can say that the spring-loaded SCV has better performance when vibration and fluttering is a concern, but this is not absolute true, because the spring itself does cause sort of vibration during the overall closure of the SCV, especially at larger stiffness values, Figure 13.

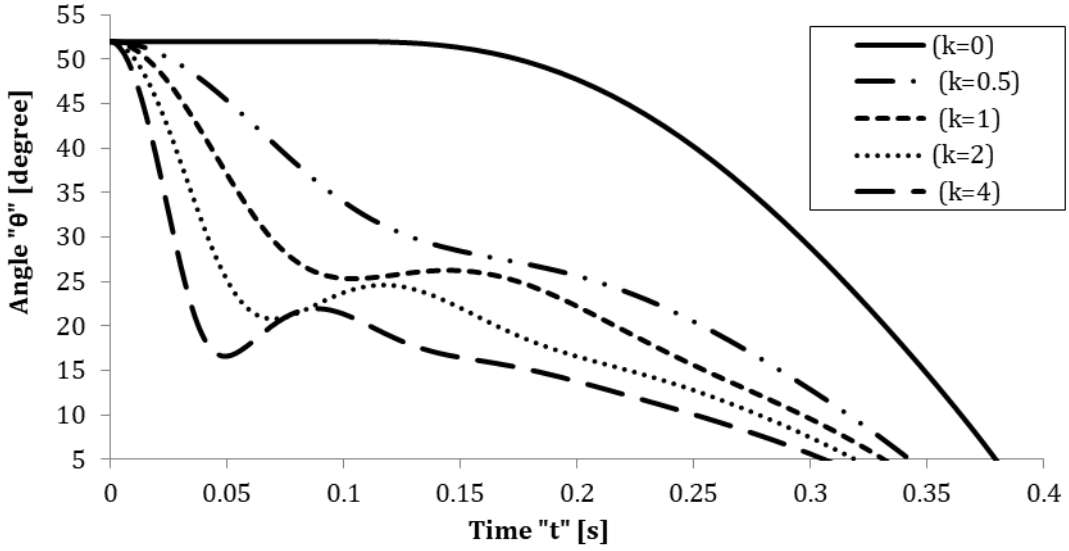

Figure 13. Closing performance at different spring stiffness values.

Figure 13, shows the effect of spring on the valve closing time and flapper's vibration, where equipping the SCV with a spring will cause some disturbance in closing regime at angles where the spring torque decreases (at smaller closing angles) and the hydraulic torque increases and dominates over the spring and the weight torques.

7. Conclusion

Check valves are important devices in any hydraulic system, the swing check valve (SCV) type has a relatively high valve flow coefficient, low pressure drop, less maintenance need and simple construction. One of the common maintenance problems of the SCV is the wear in the hinge that pivots the flapper above the flow path, the major cause of that wear is the vibration/fluttering of the flapper, which is due to operating the SCV at flow velocities less than the flow velocity required to fully open the valve without fluttering (v_{min}). Vibration may be also due to the response action of the flapper when changing the flow velocity through the valve at different operating conditions.

A new mathematical model that is validated with experimental data is introduced to avoid the past deficits of both explicit and implicit models. It can predict both steady-state and transient performance of the SCV with reliable accuracy. The introduced mathematical model formulate and quantify different valve coefficients without the need for pre calculation of these coefficients experimentally or with CFD. The new mathematical model is used to study the dynamic response of both spring-free and spring-loaded SCV at different flow velocities. Results show that the larger is the inlet flow velocity, the larger is the overshoot, the decay ratio, the settling time, and the smaller the damping ratio, i.e. the higher is the vibration and fluttering thus the wear in the SCV.

Comparison between the spring-free and the spring-loaded SCV shows that the spring reduces the transient response even at higher flow velocities, because the spring has some kind of damping effect on the flapper's vibration. On the other hand, the spring itself causes some additional fluttering in the transient overall closure, which requires some kind of optimization of each specific case study to can decide if using a spring-loaded SCV is better than the spring-free SCV, and what value of the spring stiffness should be used.

Nomenclature

A	Area, m^2
C_D	Drag coefficient
D	Disc diameter, m
f	Frequency, Hz
DR	Decay ratio
I	Moment of inertia, $km.m^2$
K	Spring stiffness, N.m/rad.
L	Distance between valve hinge and disc center of gravity, m
m	Mass, kg
OS	Overshoot
T	Torque, N.m
Ts	Settling time, s
t	Time, s
v	Flow velocity, m/s
W	Weight, N
Greek Letters	
α	Angular acceleration, $rad./s^2$
γ	Specific gravity
ζ	Damping coefficient
θ	Valve disc opening angle, rad.
ρ	Density, kg/m^3
Subscripts	
add	Added mass
$Flap$	Flapper
$fric$	Friction
$full$	Fully opening
H	Hydraulic
min	Minimum
$proj$	Projected
rel	Relative
sp	Spring

References

[1] M. Johnson, "The Misunderstood Check Valve," *Valve Manufacturers Association.*, 2006.
[2] K. L. Mcelhaney, "An Analysis of Check Valve Performance Characteristics Based on Valve Design," *Nucl. Eng. Des.*, vol. 197, no. 2000, pp. 169–182, 2000.

[3] F. A. Bensinger, "Check Valve Sizing and Selection," *flowserve*, 2009.
[4] C. Wei and X. Jing, "A Comprehensive Review on Vibration Energy Harvesting : Modelling and Realization," *Renew. Sustain. Energy Rev.*, vol. 74, no. February, pp. 1–18, 2017.
[5] D. Marques, D. A. Pereira, M. Y. Zakaria, and M. R. Hajj, "Power Extraction from Stall-Induced Oscillations of an Airfoil," *J. Intell. Mater. Syst. Struct.*, vol. 7, pp. 1407–1417, 2017.
[6] M. Y. Zakaria, M. Y. Al-haik, and M. R. Hajj, "Experimental Analysis of Energy Harvesting from Self-Induced Flutter of a Composite Beam," *Appl. Phys. Lett.*, no. July, pp. 1–6, 2015.
[7] S. Malavasi, G. Ferrarese, and M. Rossi, "A Control Valve for Energy Harvesting," in *16th conference on water distribution analysis*, 2014, vol. 89, pp. 588–594.
[8] A. A. Alothman, M. Y. Zakaria, M. R. Hajj, and S. F. Masri, "Use of Thermoelectric Generator for Water Flow Metering," *Appl. Phys. Lett.*, vol. 109, no. 03, 2016.
[9] W. J. Rahmeyer, "Sizing Swing Check Valves for Stability and Minimum Velocity Limits," *J. Press. Vessel Technol.*, vol. 115, no. November 1993, 1993.
[10] K. K. Botros, B. J. Jones, and O. Roorda, "Effects of Compressibility on Flow Characteristics and Dynamics of Swing Check Valves—Part I," *J. Press. Vessel Technol.*, vol. 119, no. May 1997, pp. 192–198, 1997.
[11] H. Lim, J. Park, and S. Jang, "Development of a Swing Check Valve Model for a Low Velocity Pipe Flow Prediction," *Nucl. Eng. Des.*, vol. 236, pp. 1051–1060, 2006.
[12] G. Li and J. C. P. Liou, "Swing Check Valve Characterization and Modeling During Transients," *J. Fluids Eng. ASME*, vol. 125, no. November 2003, pp. 1043–1050, 2003.
[13] Z. Pandula and G. Halász, "Dynamic Model for Simulation of Check Valves in Pipe Systems," *Period. Polytech. ser. Mech. Eng*, vol. 46, no. 2, pp. 91–100, 2002.
[14] P. D. Tran, "Pressure Transients Caused by Tilting-Disk Check-Valve Closure," *J. Hydraul. Eng. ASCE*, pp. 1–10, 2015.
[15] M. Turesson, "Dynamic Simulation of Check Valve Using CFD and Evaluation of Check Valve Model in RELAP5," Chalmers University of Technology, Göteborg, Sweden, 2011.
[16] E. Boqvist, "Investigation of a Swing Check Valve Using CFD," Linköping University, Sweden, 2013.
[17] C. Björk, "3D-Modeling of Swing Check Valve with Connection to Dynamic Behavior Used in System Studies," Lund University, Sweden, 2015.
[18] E. Eriksson, "CFD Study of a Pump Trip in a Pump-Check Valve System," Umeå University, Sweden, 2016.
[19] G. Vavassori, "Swing CheckValve Characterization : 3D CFD Validation of One Dimensional Models Used in RELAP5," KTH Royal Institute of Technology, Stockholm, Sweden, 2017.